J|A|C|S COMMUNICATIONS

Published on Web 02/26/2009

A Dianionic Phosphorane Intermediate and Transition States in an Associative A_N+D_N Mechanism for the RibonucleaseA Hydrolysis Reaction

Brigitta Elsässer,* Marat Valiev, and John H. Weare

Chemistry and Biochemistry Department University of California—San Diego, La Jolla, California 92093 and William R. Wiley Environmental Molecular Sciences Laboratory, Pacific Northwest National Laboratory, Richland, Washington 99352

Received October 7, 2008; E-mail: elsaesse@mail.upb.de

Calculations supporting the presence of a stable dianionic phosphorane intermediate in the hydrolysis step of the RNaseA enzyme mechanism are reported. The theoretical methods that led to the unexpected stability of this species were based on a considerably more accurate representation of the reaction process than previous calculations (see Supporting Information, SI and below). In particular accurate and comprehensive optimization of reaction pathways and free energy profiles were provided using recently implemented QM/MM methodology. This included an accurate description of quantum mechanical effects by an *ab initio* representation of a large active site region and a reliable treatment of the surrounding protein matrix at the classical MM level using a well established force field (see SI).

The RNaseA enzyme efficiently hydrolyzes phosphodiester linkages in RNA.[1] This enzyme system has been studied for over 50 years and is the best characterized ribonuclease. Yet there remains considerable debate concerning the nature of the structures of the transition states (TSs) along the reaction path. Most of the controversy concerns the structure of the TSs and their protonation states.[1−3] The putative cleavage mechanism (PM) proceeds in two steps (Scheme 1S, in SI).[1] The first step involves a transesterification reaction at the O5′ of the RNA backbone leading to the formation of an O2′, O3′ cyclic monophosphate and O5′ H terminated RNA fragments. The focus of our work is on the second step (Scheme 1 and 1S) in which the O2′−P bond in the cyclic monophosphate is hydrolyzed to form an O3′−P monophosphate. In the putative hydrolysis step (Scheme 1S) it is assumed that the reactions in both steps pass through an associative trigonal bipyramid (TBP) transition state (TS).[1−3]

The question of the possible presence of stable intermediates in phosphoryl transfer reactions has been actively debated for many years.[1−3] There are a large number of studies of the hydrolysis of cyclic and noncyclic phosphodiesters in homogeneous media (analogues of the RNaseA hydrolysis reaction) which have been interpreted in terms of the existence of a stable phosphorane intermediate along the reaction path.[4−7] In these proposed mechanisms the protonation of the phosphorane species (e.g., dianionic vs monoanionic etc.) plays a central role in its stability and the outcome of these reactions.[7] It has been proposed that without proton transfer no stable intermediate is formed.[1−7] Support for the need of protonation in the formation of the intermediate calculations has also been given by prior theoretical results (SI).

In the RNA hydrolysis reaction the lack of an O3′ isomerized product provides additional evidence that there is no stable intermediate.[6,7] However, the computational results presented here find a stable unprotonated (dianionic) intermediate along the optimized reaction path (an A_N+D_N mechanism).[2,3] The possibility of a stable phosphorane intermediate in other enzyme reactions has also been the subject of active recent controversey.[8−13]

Scheme 1. Reaction Mechanism for the RNaseA Hydrolysis of the Cyclic Phosphate

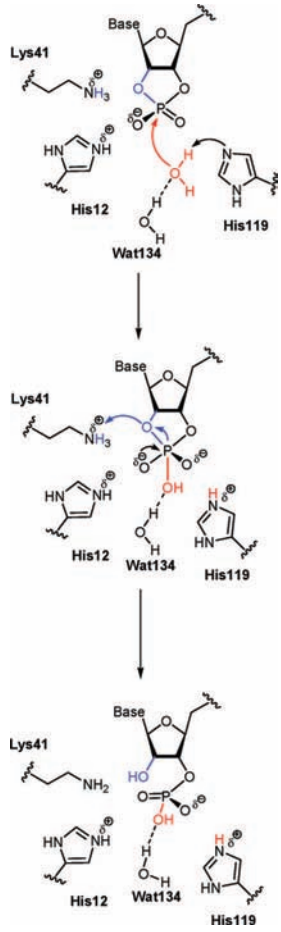

Calculations presented in this work were performed using an NWChem QM/MM module.[14,15] Initial structural input for our calculations came from X-ray[16] and neutron scattering[17] measurements of a vanadate complex generally accepted as a transition state analogue for the hydrolysis reaction. The system was divided into a region to be treated with quantum mechanical methods, the QM region, and the remaining protein, counterions, and solvent molecules described using a molecular mechanics model, the MM region (more detail is included in the SI). The forces in the QM subsystem were calculated at the B3LYP[18,19] level using the Ahlrichs-pVDZ[20] basis set. The MM region was described using the AMBER99 force field. The bonds between the QM and MM subsystems were capped with H-atoms. Two different definitions

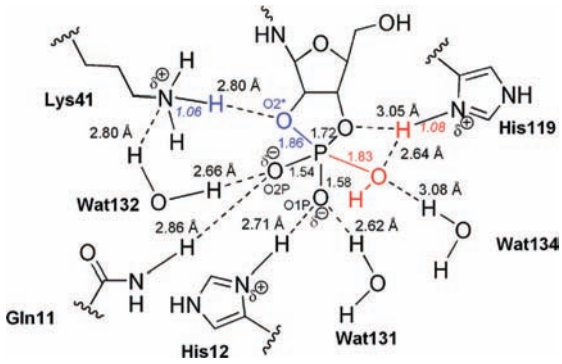

Figure 1. Stable phosphorane intermediate.

of the QM region were utilized as will be explained below. The MM region contained the remaining protein and 8790 solvating waters (SI).

To initiate the calculations the entire solvent−enzyme−vanadate structure was equilibrated by performing a series of molecular dynamics runs for 100 ps at temperatures 50, 150, 200, 250, and 298.15 K with fixed positions of the atoms in the QM region.[14] The latter contained UVC (uridyl vanadate) and fragments of the residues known to strongly effect the efficiency of the reaction[1] including Lys41, His12, His119, Gln11, Phe120, and Asp121 (a total of 99 atoms). After the equilibration stage the structure was optimized using a multiregion optimization algorithm as implemented in NWChem (see SI). This method performs a sequence of alternating optimization cycles of the QM and MM regions. Several cycles of this optimization were carried out until convergence was obtained. QM/MM optimization of the vanadate complex led to a structure showing excellent agreement (Figure 1S) with experimental structural data (rmsd 0.752 Å for the α carbon atoms (CA)) and validating the reliability of our theoretical description. The optimized vanadate complex was used in the preparation of the native system with a phosphorus atom replacing the vanadium. This calculation utilized the same definition of the QM region. To allow the system to reorganize and to avoid being trapped in a metastable minimum we equilibrated the phosphorane enzyme−substrate complex prior to QM/MM optimization of the entire system. The analysis of the resulting structure indicates that the protein backbone structure changed very little; the calculated rmsd (for the CA atoms) was 0.2916 Å. The main changes were observed in bond lengths in the active site caused by the replacement of the vanadium by the phosphorus. The associated bipyramid phosphorane intermediate structure was found to be stable (see Figures 1 and 2S) and consistent with a tightly associated phosphorane structure.

The apical bonds are 1.83 and 1.86 Å (giving a total bond order (BO)[21] of ∼1.5M), slightly shorter than those that have been recently reported for the putative phosphorane structure in the reaction mechanism for phospholipase[9] (1.83 and 1.96 Å), but longer than the equatorial single PO bond lengths (average. 1.61 Å, Figures 1 and 2S). The structure of Figure 1 is formally dianionic. Results of prior calculations (SI) propose that a dianionic species cannot exist without neutralization during the reaction because of the high charge localization. However, we note from Figures 1 and 2S that there are many H-bonds with the active site amino acid residues and water molecules that may stabilize the phosphorane structure including seven short H-bonds (O−H−O distance < 2.7 Å).

A monoanionic complex could potentially be formed by a proton transfer to an equatorial O from the acidic (protonated, NE) site of His12, Figure 1. Our calculations, however, do not support this structure. All the optimization attempts to move the proton from His12 to the O1P resulted in the return of proton to His 12 as in the dianionic structure. These results are consistent with neutron scattering[17] data for the dianionic vanadate structure.

Table 1. Energetics (kcal/mol) of the Reaction Process[a]

	TS1	INT	TS2	PS
E_{QM}	2.85	0.59	11.63	−16.51
E_{MM}	1.11	1.62	1.59	11.07
$E_{QM/MM}$	3.96	2.21	13.22	−5.44

[a] All energies in kcal/mol units referenced to the energy of the reactant complex.

To reduce the computational expense associated with the *ab initio* description of the QM region, a smaller QM partitioning scheme was utilized in the calculation of the reactant to product reaction pathway. The QM region in this case contained fragments of the His12, Lys41, His119 residues and three additional waters that were in close proximity to the reaction center in the X-ray structure (a total of 68 atoms). The effect of this smaller QM partitioning scheme was tested through the optimization of the phosphorane intermediate state and did not effect the structure significantly (differences in bond lengths were less than 0.1 Å).

Based on the structure of the stable intermediate phosphorane complex (see Figure 1), we have optimized reactant and product states from initial trial structures constructed from the intermediate, Figure 1, by lengthening of the P−O3P bond and lengthening of the O2′−P bond, respectively. The reaction pathways from the reactant to the intermediate and from the intermediate to the product state were obtained using a QM/MM nudged elastic band (NEB) methodology.[14,22] In the NEB calculations a total of 2 × 8 beads/replicas were used for the pathway representation in two separate calculations toward the reactant and product state starting from the intermediate structure. The initial guess for the pathway was generated by linear interpolation between the optimized reactant, intermediate, and product states. The system was equilibrated at each NEB node (including the reactant and product states) allowing the remaining protein and the solvent to respond to the movement along the reaction coordinates.[14]

To properly account for finite temperature fluctuations of the protein and solvent, thereby, providing accurate estimation of activation barriers, the Helmholtz free energy along the reaction paths was calculated. Transition state complexes were identified as maxima along the free energy paths. Results of these calculations are summarized in Table 1 and Figure 5S. In the near in-line reaction path from the reactant state to the intermediate the system passes through, TS structure TS1, Figures 2a and 6S (barrier height 3.96 kcal/mol), to the intermediate (INT), Figures 1 and 2S, stable by 2.21 kcal/mol (Figure 6S). After the INT the reaction coordinate passes through a much higher maximum, TS2 (barrier height 11.01 kcal/mol), Figures 2b and 7S, and onto the product state. The overall activation barrier (energy to surmount TS2 from the reactant state) of 13.22 kcal/mol and the total free energy change of −5.44 kcal/mol are in good agreement with observations (19 and −4 kcal/mol).[1] Exact analysis of the protein contributions to the energetics of the reaction process is complicated due to the fact that the QM region already contains part of the protein. Still we can observe (see Table 1) that the classical energy of the distant protein environment (E_{MM}[23]) contributes significantly throughout the reaction process with a pronounced destabilization contribution to the product state.

The INT, TS1, and TS2, Figures 1 and 2a,b, may all be characterized as TBP with very nearly planar equatorial atoms and

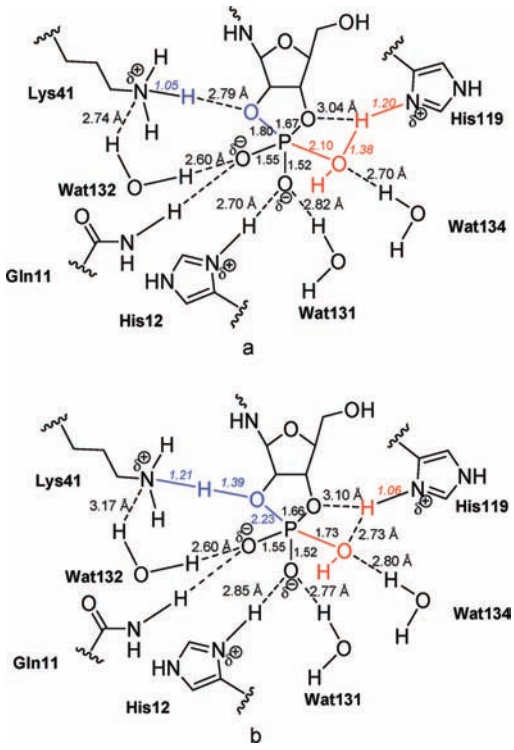

Figure 2. TS1 (a) and TS2 (b).

longer apical bond directions perpendicular to the equatorial plane. The cyclic phosphorane in all three structures contains one equatorial and one apical bond consistent with a conjecture of Westheimer.[23] In the path from the reactant through transition state TS1 to the intermediate the nucleophilic species (OH^- colored red in Figure 1) resulting from the concerted transfer of the water proton to His119 attacks the phosphorus. In TS1 the H-bond to the His119 is very short, 2.54 Å, although the transfer of the proton is not complete (His119−H bond order of 0.26). The P−O3P bond has not been formed, with a calculated bond order of 0.11 (see also Figure 6S).

The barrier to the product from the INT state (Figure 1) through TS2 (Figure 2b) is considerably higher than the barrier on the reactant side. In the structure of TS2, Figures 2b and 7S, the proton transfer from the Lys41 hydrogen has not yet occurred (Lys41−H bond order is 0.87). However, the apical bond to the leaving oxygen is nearly broken (P−O2′ bond order is 0.28).[21,24] As illustrated by their positions in INT, TS1, and TS2 and in Scheme 1, the waters included in the calculation may stabilize the structures along the reaction coordinate (e.g., the very short O1P−Wat132 H-bond of 2.66 Å, Figure 2S). The movement of Wat134 is highly coordinated with the attacking water.

In Scheme 1 (these calculations) Lys41 donates the proton in the final phase taking the role of His12 in the PM as the catalytic acid. As noted by other workers,[25] in the vanadate X-ray structure the Lys41 is in a better position to donate a proton (coordinates O2′) than His12 (coordinating O1P, 1S and Figure 2). To check the stability of the protonation in our product state, we forced the proton to be transferred in the path from the intermediate state to the product from His12 to O2′ leaving the Lys41 protonated. This resulted in an energetically unfavorable product.

Additional support for this mechanism comes from docking calculations (discussed in SI). The objective of these calculations was to try to find an enzyme−substrate docking in which the roles of Lys41 and His12 were reversed as in the PM. The RNaseA X-ray structure (1RUV) with UVC removed from the active site and with the cyclic TBP phosphorane docked into the catalytic pocket was used to initiate the calculation. The active site residues were allowed to move, and the energetics of the various structures generated by moves of the docking algorithm were evaluated (SI). While a substantial effort was made to find an intermediate ligand structure corresponding to the PM, none was found. Rather, the best docking structure fit well with the optimized structure of our intermediate, Figure 8S and Table 2S. Similar docking calculations were done for the product state. In this case as well, a docking structure in close agreement with our product structure was found. No structure consistent with the PM was identified.

Because of the high level of these calculations which includes an accurate quantum chemical treatment of the interactions in the catalytic active site of the system and a tested molecular mechanics description of the remaining enzyme and solvent, an optimized reaction path, as well as thermal averaging (free energy estimates), we believe that the results presented here provide strong support for the presence of a stable phosphorane intermediate in this important catalytic mechanism. The additional elements included in this calculation contributed to the unexpected stability of this species and may be important to the interpretation of other enzyme mechanisms.

Acknowledgment. The authors would like to acknowledge DAAD for the financial support of B.E. and ONR for the financial support of M.V. Calculations were carried out at the MSCF in the EMSL user facility sponsored by the U.S. DOE.

Supporting Information Available: Calculation details, optimized, transition state and docking structures. This material is available free of charge via the Internet at http://pubs.acs.org.

References

(1) Raines, R. T. *Chem. Rev.* **1998**, *98*, 1045–1065.
(2) Hengge, A.; Onyido, I. *Curr. Org. Chem.* **2005**, *9*, 61–74.
(3) Perreault, D.; Anslyn, E. *Angew. Chem., Int. Ed. Engl.* **1997**, *36*, 432–450.
(4) Breslow, R.; Dong, S. D.; Webb, Y.; Xu, R. *J. Am. Chem. Soc.* **1996**, *118*, 6588–6600.
(5) Gerratana, B.; Sowa, G. A.; Cleland, W. W. *J. Am. Chem. Soc.* **2000**, *122*, 12615–12621.
(6) Sowa, G. A.; Hengge, A. C.; Cleland, W. W. *J. Am. Chem. Soc.* **1997**, *119*, 2319–2320.
(7) Kluger, R.; Covitz, F.; Dennis, E.; Williams, L.; Westheim, F. *J. Am. Chem. Soc.* **1969**, *91*, 6066–&.
(8) De Vivo, M.; Del Peraro, M.; Klein, M. L. *J. Am. Chem. Soc.* **2008**, *130*, 10955–10962.
(9) Leiros, I.; McSweeney, S.; Hough, E. *J. Mol. Biol.* **2004**, *339*, 805–820.
(10) Baxter, N.; Olguin, L.; Golicnik, M.; Feng, G.; Hounslow, A.; Bermel, W.; Blackburn, G.; Hollfelder, F.; Waltho, J.; Williams, N. *Proc. Natl. Acad. Sci. U.S.A.* **2006**, *103*, 14732–14737.
(11) Knowles, J. *Science* **2003**, *299*, 2002–2003.
(12) Lahiri, S. D.; Zhang, G. F.; Dunaway-Mariano, D.; Allen, K. N. *Science* **2003**, *299*, 2067–2071.
(13) Webster, C. *J. Am. Chem. Soc.* **2004**, *126*, 6840–6841.
(14) Valiev, M.; Yang, J.; Adams, J. A.; Taylor, S. S.; Weare, J. H. *J. Phys. Chem. B* **2007**, *111*, 13455–13464.
(15) Valiev, M.; Garrett, B. C.; Tsai, M. K.; Kowalski, K.; Kathmann, S. M.; Schenter, G. K.; Dupuis, M. *J. Chem. Phys.* **2007**, *127*, 051102.
(16) Ladner, J. E.; Wladkowski, B. D.; Svensson, L. A.; Sjolin, L.; Gilliland, G. L. *Acta Crystallogr., Sect. D* **1997**, *53*, 290–301.
(17) Wlodawer, A.; Miller, M.; Sjolin, L. *Proc. Natl. Acad. Sci. U.S.A.* **1983**, *80*, 3628–3631.
(18) Becke, A. D. *J. Chem. Phys.* **1993**, *98*, 5648.
(19) Lee, C.; Yang, W.; Parr, R. G. *Phys. Rev. B* **1988**, *37*, 785.
(20) Schafer, A.; Horn, H.; Ahlrichs, R. *J. Chem. Phys.* **1992**, *97*, 2571.
(21) Mildvan, A. S. *Proteins: Struct., Funct., Genet.* **1997**, *29*, 401–416.
(22) Henkelman, G.; Jonsson, H. *J. Chem. Phys.* **2000**, *113*, 9978–9985.
(23) Westheimer, F. H. *Acc. Chem. Res.* **1968**, *1*, 70–78.
(24) Berente, I.; Beke, T.; Naray-Szabo, G. *Theor. Chem. Acc.* **2007**, *118*, 129–134.
(25) Messmore, J. M.; Raines, R. T. *J. Am. Chem. Soc.* **2000**, *122*, 9911–9916.

JA807940Y